



Electrocardiogram Waveform Acquisition

Author

Daniel ELABD

Student Number

17074529

Supervisor

Dr. SHIRAZ

Second Supervisor

Prof. RODRIGUES

April 21, 2020
A BEng Project Final Report

Declaration

I have read and understood the College and Department's statements and guidelines concerning plagiarism.

I declare that all material described in this report is all my own work except where explicitly and individually indicated in the text. This includes ideas described in the text, figures and computer programs.

Name: Daniel Elabd

Signature: Daniel

Date: April 22, 2020

Contents

1	Introduction	3
1.1	Goals and objectives	4
1.2	Developed wireless ECG sensors	4
2	Supporting Theory	6
2.1	The generation & characteristics of ECG signals	6
2.2	Clinical 12-lead ECGs	9
2.3	Biopotential amplifiers	10
2.4	AC coupled inputs	12
2.5	Instrumentation amplifiers	13
2.6	ECG noise and filtering	14
2.7	Driven Right Leg (DRL) circuit	15
2.8	Electrodes for ECG	17
3	Methods	20
3.1	Biopotential amplifier design	20
3.2	PCB design and miniaturisation	22
3.3	Shielding and testing	23
3.4	Lab setup	24
4	Results and Analysis	25
4.1	ECG recordings	25
4.2	Discussion	26
5	Future work	28
6	Conclusion	30
A	Tested PCB, 2 layer (computer design)	32
B	Manufactured PCB (previous version)	33
C	Miniaturised PCB, 4 layer (computer design)	34
D	Miniaturised PCB without BNCs (actual amplifier size)	36

Abstract

A miniaturised PCB design for a low-power, bipolar, biopotential amplifier is presented in order to, in future, develop a completely wireless, compact ECG amplifier suitable for long term monitoring to accurately record the local ECG signal for clinical applications. Micro-power and micro-size components are used for the proposed biopotential amplifier. Most approaches towards creating wireless ECG amplifiers include wiring and may not be approved for clinical use. The system to be developed involves a mini PCB approximately the size of a USB stick to record the ECG signal which when placed on the body surface, will immediately record and wirelessly transmit the ECG signal, eliminating the need for any wiring. A biopotential amplifier was developed and successfully recorded the ECG signal showing all significant characteristics of the ideal waveform. The design was miniaturised on a PCB of dimensions 3.5x5cm. Using this, a complete system consisting of a fully wireless, compact ECG device can be realised and developed in future for clinical applications hence allowing for comfortable long term monitoring of subjects.

1 Introduction

Electrocardiograms (ECGs) have been around since the end of the 19th century, changing the bioelectronics field ever since. ECGs play a vital role in both the healthcare and fitness sectors [1]. The clinical 12-lead ECGs in hospitals are used to diagnose a wide range of cardiovascular diseases including arrhythmias, hypertension (high blood pressure) and myocardial infarctions (heart attacks) [2], therefore being of great significance to the medical field. The 12-lead ECG however requires 10 electrodes (10 wires) to be attached in different areas on the patient's body hence introducing limitations. The process of setting up is time consuming. The wiring limits the patient's freedom of movement, which is a more significant problem where long-term monitoring is essential. Holter monitors are small, wearable devices which are used for remote ECG monitoring and allow for patient movement, however they are uncomfortable for the patient, especially for long periods of time. There are also further monitoring/technical limitations involved with Holter monitors as described in [3], [4] and [5].

ECGs are also used in the fitness sectors to monitor heart activity during exercise for analysis and studies, for example analysing pre- and post-exercise ECG recordings such as the study conducted

in [6]. Therefore, there is an increasing interest in developing a compact ECG sensor which would allow for such applications.

1.1 Goals and objectives

The proposed project hence aims to develop a miniaturised, low-power, bipolar biopotential amplifier that will record, as accurately as possible, the local ECG signal for clinical use. The ideal size of the amplifier PCB is approximately 2x3 cm (about the size of a small USB stick). It should also have a 24-hour battery life therefore minimum power consumption is required.

In future, the system is to be integrated with wireless technology allowing for patient comfort and freedom of movement for long-term monitoring. It should offer ease of use, where the subject is to place the amplifier on the appropriate location and the device would instantly record and wirelessly transmit the ECG signal to a computer. Additionally, the system should also allow for movement such as walking, running and other general exercises.

1.2 Developed wireless ECG sensors

These limitations inspired the development of wireless ECGs which attempt to introduce more patient freedom and allow for long-term monitoring. There is, however, the problem of achieving a similar level of ECG accuracy as that associated with the conventional wired 12-lead system. One attempt nevertheless successfully implemented the "design of a wearable 12-lead non-contact electrocardiogram monitoring system" [7] in 2019. This approach (which uses non-contact or capacitively coupled electrodes (CC-ECG), discussed in section 2.8), successfully achieved high correlation against the conventional 12-lead setup with conductive gels. Results were also achieved whilst patients were walking, although motion artefact caused the slight baseline swinging of the ECG signals.

Researchers at Aachen University in Germany also developed a similar approach [8] (also 12-lead). They used conductive textiles integrated in a shirt to replace standard gel electrodes hence creating an ECG shirt that patients can wear instead of using the Holter monitor. The shirt was tested and validated against a commercial Holter monitor and successfully obtained high correlation. Results were also validated against the conventional 12-lead setup during 3 scenarios: lying, sitting and walking. The P-wave demonstrated a lower correlation while walking, and the T-wave lower correlation for the 3 scenarios. The P, Q, R and S-waves all demonstrated a corre-

lation higher than 0.9 for the remaining scenarios. From these results it was concluded that the shirt is suitable for 12-lead ECG recordings and provides more patient comfort and freedom.

There are lots of developments towards creating more compact and flexible ECG sensors, which involve the use of fewer leads. Researchers at McMaster University developed a low-power, two-lead wireless ECG sensor using capacitively coupled electrodes [9]. The system was integrated into a shirt to be worn by patients where there were two chest electrodes and one reference electrode placed on the hip. From the conducted tests it was found that the signal obtained from the capacitive electrodes (after processing) was of weaker amplitude and of higher susceptibility to noise than the signal obtained from using gel electrodes. However, important intervals and peaks such as the QRS complex and P- and T-waves were clearly observed and easily interpreted by a cardiologist. The proposed system has very-low power consumption and is comfortable, hence allowing for long-term monitoring. The paper cited also provides a table comparing the advantages and disadvantages of several other ECG sensor systems developed.

'An ultra-high input impedance ECG amplifier for long-term monitoring of athletes' [10] was developed by researchers at the University of Naples and the University of Sydney. The sensor has wireless connectivity and uses capacitively coupled electrodes (made from conductive rubber) for long-term monitoring of athletes undertaking different forms of exercise. While the athlete was at rest, the correlation between the ECG signal recorded using their proposed electrodes and that associated with the use of normal gel electrodes was always greater than 0.96. Being compared against a clinically approved monitoring device, the sensor also recorded a good quality ECG signal for exercises such as bench presses, squatting and even in the case when the athlete was swimming (fully submerged underwater). The amplifier had minimal power consumption and therefore could monitor subjects for long periods of time. The team also tested the amplifier using textile electrodes (electrodes made from conductive fabric) instead of capacitive ones. However, the recorded results were not as of high quality signals as the capacitive electrodes.

Other approaches include designing an armband, such as the design developed by Vega and Wan-Young [11]. This approach also used capacitive electrodes and successfully recorded the ECG signal through different cloth materials and thicknesses.

All the cited proposed systems have used CC-ECG, where the technology has been increasingly popular. This is due to the fact that they are 'non-contact' i.e. they do not need direct contact with the

skin (can record ECG through clothes) and do not need any preparation hence making them suitable for long-term and home monitoring. Section 2.8 will discuss CC-ECG in more detail and compare them against different types of electrodes.

Moving on from CC-ECG, a system proposed in [12] includes the use of textile electrodes. It aims to provide continuous ECG monitoring of children with an increased risk of Sudden Infant Death Syndrome. The electrodes were integrated with an ECG sensor into a baby suit worn by a 12-year old baby. The use of textile electrodes displayed an ECG signal with more base line drift when compared to that using conventional gel electrodes. However, the paper claims that the signal quality was more than adequate for the required application.

Also based on textile electrodes, Ottenbacher, Römer and others [13] developed a similar system where a bluetooth ECG system was incorporated into a t-shirt. They developed a system using removable, flexible electronic systems to make the t-shirt washable and comfortable. Although no actual ECG recordings were presented, a test was conducted. It was found that a lot of signal noise was produced by variation in pressure of the electrode to the skin (due to respiration and movement) which caused baseline drift of the ECG signal. Solutions were proposed to reduce the noise but no further developments were mentioned.

The developed ECG amplifiers discussed mostly achieve the goals associated with this project, however the goal of the project is to further simplify these systems. Most systems mentioned include wiring of some form. One aim of this project is to further simplify the ECG amplifiers so that they are completely wireless. For example, when the sensor is fully developed, it should be as easy as to directly place the sensor on the appropriate location and it would immediately record and transmit the ECG signal to a computer.

2 Supporting Theory

2.1 The generation & characteristics of ECG signals

2.1.1 Physiology of the human heart

The human heart consists of four compartments, the right and left atria and ventricles, with walls composed of cardiac muscle known as the myocardium. The orientation of the heart is such that the right ventricle is nearer to the front of the body while the left atrium is

nearer to the back of the body. This orientation has a significance in the electric function of the heart [14].

In a normal cardiac cycle, the atria and ventricles contract and relax. The sinoatrial (SA) and atrioventricular (AV) nodes are a group of cells in the myocardium. These cells, along with others, generate electrical impulses throughout the myocardium, [15]. As a result of these impulses, polarisation and depolarisation of cell membranes occurs in the atria and ventricles. Therefore, there are resultant 'cardiac vectors' which represent the polarisation and depolarisation of the different regions of the heart, as illustrated in figure 1. Each cardiac vector contributes to constructing the ideal ECG signal shown in figure 2.

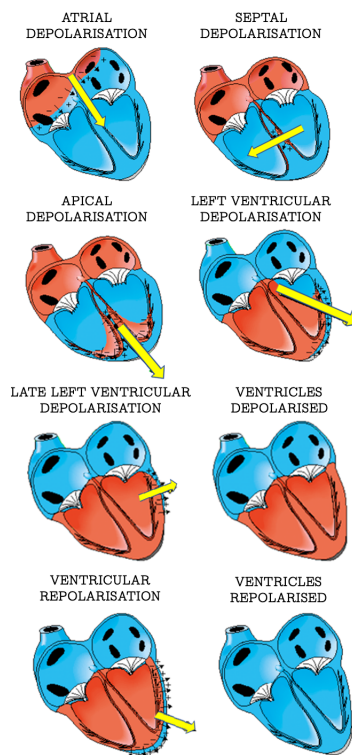


Figure 1: Cardiac vectors representing polarisation and depolarisation of the atria and ventricle chambers. Figure from [14].

2.1.2 ECG waveform characteristics

As shown in figure 2, the waveform has several deflections. The first deflection is the P-wave which represents atrial depolarisation. Atrial

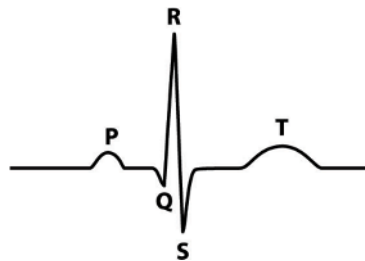


Figure 2: Ideal ECG waveform

muscle cells then repolarise, but this is too insignificant to be detected by electrodes and therefore does not appear in the ECG waveform. The second deflection, being the largest peak, is known as the 'QRS complex' and represents the ventricular muscle cell depolarisation. The T-wave hence shows the ventricular repolarisation, which is large enough to be detected unlike atrial repolarisation [15].

All the peaks in the waveform shown each have a large significance in analysing ECGs and diagnosing cardiovascular diseases. For example, a wide QRS complex indicates ventricular enlargement (hypertrophy, meaning the myocardium becomes abnormally thick) [15].

To further understand the nature of ECG signals, figure 3 shows us a graph of the typical amplitudes and frequencies of different bio-signals. For ECG, the typical amplitude ranges from approximately 10^{-4} V to 10^{-2} V. The frequency ranges from approximately 10^{-2} Hz to 10^2 Hz.

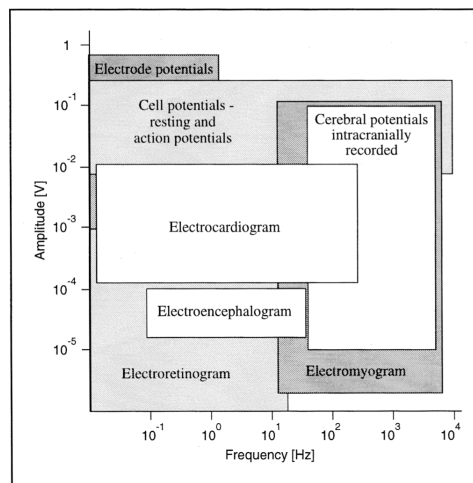
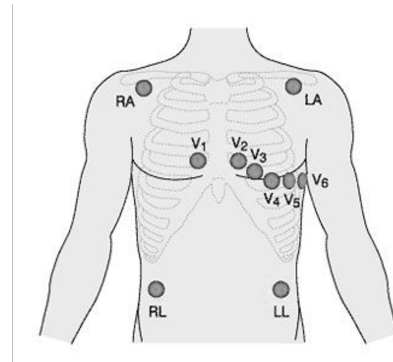


Figure 3: electrical properties of different bio-signals. Figure from [16].

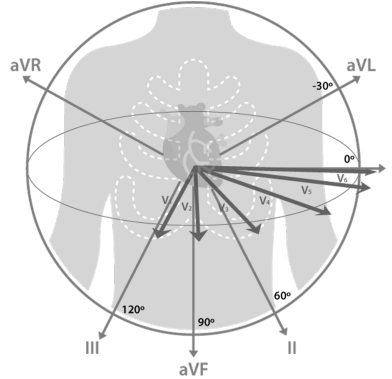
This background is essential to understanding the significance of each aspect of the ECG signal and the appropriate manipulation of the signal that is based on its electrical properties.

2.2 Clinical 12-lead ECGs

Clinical 12-lead ECGs are used in hospitals to record the ECG signal, gathering information from 12 different areas of the heart. This is done using 10 electrodes that are placed on specific parts of the body (limbs and chest) using both the vertical and horizontal heart electrical planes. Figure 4 shows us the electrodes placement and the 12-leads for further clarification.



(a) The 10 electrodes placement. Figure from [17]



(b) ECG 12-leads obtained from 10 electrodes.
Figure from 'Cables and Sensors'

Figure 4: 12-lead ECG electrode placement and lead vectors

Figure 4a shows us where the 10 electrodes are placed. The limb leads RA, LA, RL and LL stand for right arm, left arm, right leg and left leg. Figure 4b shows us the 12-lead vectors and their correspond-

ing names. Leads I, II, III, aVR, aVL, aVF are all vertical plane leads (known as frontal leads). Leads V₁ to V₆ are in the horizontal plane (known as transverse leads). All the leads are unipolar except for leads I, II and III which are bipolar (i.e. require a positive and negative electrode). Using three limb electrodes (RA, LA and LL) we obtain 6 leads, for example, lead I would be placing the positive electrode on the LA, the negative electrode on the RA and the reference electrode on the LL. Leads II and III would be obtained using different arrangements. The remaining limb lead RL is the reference electrode (further discussed in section 2.7). The chest leads provide the remaining six, hence a total of 12-leads. This setup is known as Einthoven's lead system. The variation of the different lead vectors and planes therefore record the corresponding electrical activity of the cardiac vectors shown in section 2.1 (figure 1) and with these different perspectives of the heart's activity the resulting ECG signal is recorded. The end result is the waveform obtained from each lead, meaning that there will be 12 waveforms recorded (unlike this project where the local ECG signal is recorded, i.e. one waveform), each with a significance in identifying different types of cardiovascular disease.

Since there are 10 electrodes, the process is time consuming (set-up wise) and is a hassle; it can be seen that it limits patient freedom and is unsuitable for long-term monitoring. The proposed project aims to record the *local* ECG signal using a bipolar amplifier to allow for a system where there is more patient freedom and less hassle.

Understanding 12-lead ECG interpretation contributes to further understanding how ECG signals are recorded. Any developed system is usually compared against the 12-lead as a method of justifying whether or not the system can be approved for clinical use.

2.3 Biopotential amplifiers

2.3.1 Biopotential amplifier requirements

A biopotential amplifier is usually the first stage in any bio-signal recording system. Because of this, they are extremely critical to the system's overall performance [18]. The measurements of bio-signals, such as ECG, involve low voltage levels (as indicated in figure 3), high source impedances as well as interference and noise signals. In order to properly observe these signals, they need to be amplified. Biopotential amplifiers, therefore, need to meet specific design requirements/criteria in order to process and amplify these bio-signals properly to record and analyse them. The design requirements include appropriate amplification, rejection of noise and interference

signals and protection of equipment and patients from voltage and current surges [16].

The input signal that the biopotential amplifier sees includes several components such as the desired and undesired bio-signal components, the 50 Hz power line interference, tissue/electrode interface signals and other noise. Therefore, the amplifier should be designed such that the undesired components, interference and noise should be filtered and hence only show the desired aspects of the ECG signal.

The biopotential amplifier should also have a large common-mode rejection ratio (CMMR), meaning that the circuit should reject common-mode signals (signals that appear at both inputs of the differential amplifier, such as the 50 Hz interference). A CMMR of at least 100 dB [16] would be sufficient to reject line frequency interference. The amplifier's input impedance should be large (at least $10^9\Omega$) to prevent impedance mismatches with the electrode-skin interface which can reduce the CMMR of the circuit.

For patient safety, the design of the amplifier must have some form of isolation in order to protect the patient from any electric shock due to large currents that can flow through the electrodes.

The criteria mentioned above are essential to creating any biopotential amplifier, in the proposed project however, there are more requirements that need to be met. One requirement is that the amplifier has to be as compact as much as possible, the other being that it has to have minimal power consumption. These criteria are essential to achieving the proposed project's main goal.

2.3.2 Biopotential amplifiers design

In order to fully meet these requirements, most biopotential amplifiers usually include most of the same circuit blocks, such as the DRL circuit or high pass and low pass filters. A general structure for a biopotential amplifier is shown in figure 5. Most of the amplifiers discussed in section 1.2 are all based around most of these building blocks.

This is the general structure of most biopotential amplifiers. E1 and E2 are the two input electrodes while E3 is the reference electrode. Some alternative designs exclude AC coupling and remove DC offsets by additional suppression circuits. A gain of 500-1000 is usually sufficient for amplifying ECG signals, since a minimum amplitude of 10^{-4} V would be amplified to 0.1 V. Further amplification can be included if required by the application. The filter cut-off values included are specific to ECG signals; different designs use differ-

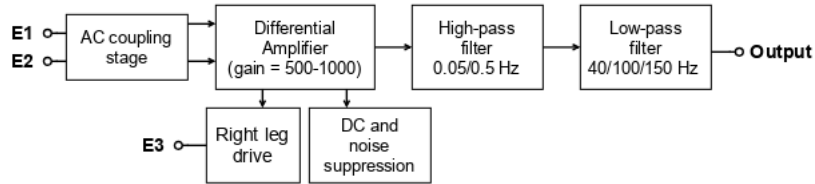


Figure 5: General biopotential amplifier block diagram

ent cut-offs. Filtering will be discussed in section 2.6. Additionally, some designs choose to incorporate isolation amplifier circuits as an extra measure of patient and device safety.

Each of these circuit blocks will be discussed in detail throughout this report. A general understanding and overview of biopotential amplifiers however is vital to understanding the significance of each block and its contribution to the project.

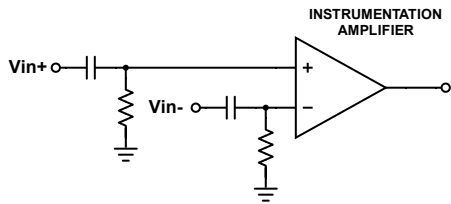
2.4 AC coupled inputs

Having an ac coupling input stage for biopotential measurements is essential. Electrode offsets can be several of magnitudes larger than the ECG signal, using a dc coupled front would limit the gain in order to prevent the amplifier from saturating [19]. Therefore, for high-gain biopotential amplifiers an ac coupled front is used. There are different types of AC coupling fronts that can be used, some of which will be discussed. There are two main methods of ac coupling, passive circuits which use blocking capacitors and active circuits which are based on closed-loop control of the dc level [19]. Figure 6 shows us some ac coupling networks.

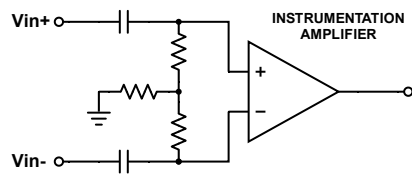
It can be seen that figures 6a and 6b include grounded resistors, which effectively degrade the circuit's common-mode rejection (CMR) [19]. Therefore, the Spinelli paper cited proposes an ac coupled front (shown in figure 6c) that does not require a grounded resistor hence achieves a large CMMR. From the transfer function of the circuit,

$$G(s) = \frac{s\tau_2}{1 + s\tau_2}$$

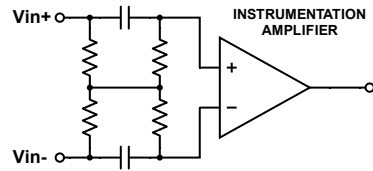
it can be seen that this ac coupled network also acts as a high-pass filter. This circuit was the one used for the ac coupling stage of this project.



(a) Basic method for ac coupling



(b) Alternative method for ac coupling



(c) Spinelli's ac coupled front

Figure 6: Different ac coupled input networks

2.5 Instrumentation amplifiers

An instrumentation amplifier (IA) is a differential amplifier that is specially designed for applications which have requirements such as high input impedance, high common-mode rejection, low noise and high gain. It is a known fact that the CMRR of IAs is much higher than that of a single-op amp differential amplifier, the reason being that the cascaded differential stages combine their respective CMRRs in some way [20]. The cited paper provides the CMRR derivations for a single-op amp differential amplifier against that of the three op-amp IA. Having a high CMRR is vital for any biopotential amplifier.

Other qualities in IAs such as high input impedance (which cannot be easily and efficiently achieved in single op-amp differential amplifiers [16]) and low noise are also requirements for biopotential amplifiers as previously discussed in 2.3.1, therefore an IA is the best option to be used in biopotential amplifiers.

2.6 ECG noise and filtering

2.6.1 Noise present in ECG signals

There are many types of noise signals present in ECG signals which need to be appropriately filtered in order to preserve the significant aspects of the waveform for proper observation and diagnosis. Types of noise arise from the power line interference, baseline wander, motion artefacts and electrode contacts. The power line interference is the 50 Hz signal which the DRL circuit suppresses as discussed in the next section (2.7).

Baseline wander (BW) is a low frequency noise component in the ECG signal and arises from respiration or from patient or instrument motion [21]. For better clinical diagnosis, the BW component needs to be filtered. Motion artefacts cause undesired signals to superimpose on the ECG signal, and are caused by a change in the potential of the skin. When the patient moves causing the skin to stretch, the skin potential decreases by 5 mV from the typical 30 mV [22] and this change is amplified and observed as artefacts. The skin-electrode resistances also introduces noise components.

2.6.2 ECG noise reduction and filtering

There are many techniques involved with suppressing the mentioned noise components in ECG signals. There is a method to reduce or suppress each type of noise mentioned above. BW artefacts are of low-frequencies and therefore one approach of removing the artefacts is the high-pass filtering of the ECG signal. However, because there are variations in the frequency spectrum of ECG signals, using a high pass filter (HPF) can distort the signal [23]. The most widely used lower cut-off frequency for the HPF is 0.5 Hz, by assuming a lower bound for heart rate equal to 30 beats per minute (bpm). Although this cut-off will remove BW, it will distort the T-waves and ST segments of the ECG signal [24]. Because of this, a cut-off of 0.05 Hz is recommended by the American Heart Association instead [25], which caused no important distortion in the ECG signal. In a paper by Buendia-Fuentes, Arnau-Vives and others [26] a comparison of results between using different low-frequency cut-offs (0.05 Hz and 0.5 Hz) and high-frequency cut-offs was studied. In this paper it was concluded that for ST segment interpretation, a value of 0.05 Hz should be used for the HPFs, as stated in [24]. This conclusion was also reached by the research in [27]. Different papers use different approaches for cut-off frequency values; the Spinelli AC-coupled front-end [19] used for this project used a HPF of cut-off 0.033 Hz.

There is another approach used to remove BW called empirical mode decomposition (EMD) which will not be discussed in this report. Where motion artefacts becomes a problem, skin abrasion is sometimes carried out to reduce its effects.

The upper cut-off frequency for ECG signals most commonly used and recommended by the American Heart Association [28] is 150 Hz, as ECG components beyond this frequency are usually unwanted and any external high frequency noise is attenuated. Other upper cut-off frequencies such as 40 Hz are also commonly used. Several papers were published and compared the use of 150 Hz against 40 Hz, such as [29] and [26]. About 1600 people underwent 12-lead ECG tracings using the two different high-frequency cut-offs. Although the recommended cut-off was 150 Hz, the results they found involved the 40 Hz cut-off resulting in an increased rate of optimal quality ECGs compared to the 150 Hz cut-off. A thorough research showing the different bandwidths used by international cardiological communities [27] showed that only 5% of the involved communities used the recommended upper cut-off of 150 Hz. The paper presents results showing that the 150 Hz causes less distortion to the S-wave and recommends using this value.

Despite the different research and claims, 150 Hz was the cut-off used in this project as it is the standardised and recommended value. Additionally, the proposed biopotential amplifier is based on the Spinelli paper previously cited [19] and used the same values for filters.

2.6.3 Suppression of DC and additional noise

There are op-amp input offset voltages which are amplified and can therefore reduce the output range of the amplifier, as well as dc voltage drops across bias resistors. On top of this, there is thermal noise arising from resistors and op-amp input voltage noise. These can be suppressed by including an integrator feedback loop around the difference amplifier as in [19]. The circuit is also a high-pass filter and is able to attenuate the unwanted noise.

2.7 Driven Right Leg (DRL) circuit

The DRL circuit is as essential circuit included in biopotential amplifiers. Biopotential measurements are very sensitive to electromagnetic interference (EMI); this circuit makes the ECG signal less prone to EMI. It suppresses the common mode signals that are derived from

the 50 Hz power line interference by providing common-mode feedback.

When a differential amplifier records a biopotential, the voltage of the patient with respect to the amplifier's common is called the common mode voltage, denoted by v_{cm} [30]. This voltage can become an interfering differential signal, therefore it is desirable to minimise it. This is done by using the reference electrode. The electrode provides a low impedance path between the patient and the amplifier common hence making v_{cm} a small value. This electrode is connected to the DRL circuit, which limits the current flowing through it so that it does not harm the patient. Although the reference electrode provides a low impedance path, poor contact can cause an impedance of around 100 k Ω [30]. The DRL circuit decreases the magnitude of this resistance. Figure 7 shows us the conventional DRL circuit schematic.

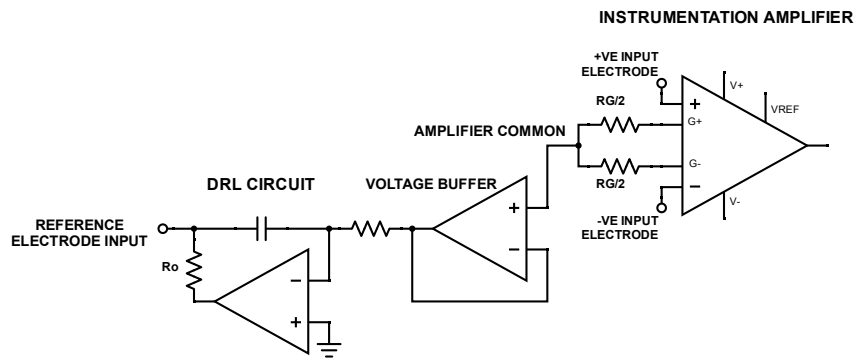


Figure 7: DRL circuit demonstration

The figure above shows us the amplifier common point which is connected to a voltage buffer (for impedance matching) and then to the DRL circuit, which is basically an op-amp integrator circuit. The instrumentation amplifier resistor R_G which controls the gain of the amplifier is split into two equal resistances each of value $R_G/2$ in order to average the voltage of the two electrodes inputs (the differential pair) and sense v_{cm} . The DRL circuit, being an inverting amplifier, amplifies and inverts v_{cm} , feeding it back to the body through the reference electrode. Therefore, the patient's body is now driven to the same voltage as the amplifier common [31], ideally driving the common-mode voltage, v_{cm} , to zero. The feedback loop therefore improves the common-mode rejection of the circuit by an amount equal to $(1 + A)$ where A is the closed loop gain of the feedback loop [32]. There is also a resistor R_o at the output of the DRL circuit which is

of high resistance to provide a large isolation impedance from the patient to ground.

2.7.1 A driving right leg circuit (DgRL)

Guermandi, Scarselli and others present a different approach to mitigate the effect of common mode signals in [33]. They propose a 'driving' right leg circuit where the potential detected by an electrode on the patient's scalp drives the IA isolated ground towards a fixed voltage. This minimises the common mode voltage v_{cm} seen at the input and will reject interference, hence improving CMR. In a DRL, negative feedback is used to provide a correction signal to minimise v_{cm} . The paper provides an analysis showing how the CMR is improved compared to that of a DRL. The DgRL was incorporated into an EEG (electroencephalogram) amplifier and successfully suppressed the 50 Hz power line interference without any further signal processing or filtering. The proposed design reduced the common-mode signal by an excess of 70 dB which is at least 30 dB more than a DRL circuit.

2.8 Electrodes for ECG

2.8.1 Different types of electrodes

There are many types of electrodes that can be used for ECG signal acquisition. These include the conventional wet electrodes, which are made of silver chloride (AgCl) material, and use electrolytic gel as a method of increasing the electrode-skin interface conductivity. They also usually require skin preparation such as shaving or alcohol cleansing. Dry electrodes however do not involve the use of gel as implied by their name. There are two types of dry electrodes; non-contact and dry contact. Dry contact electrodes consist of a single material which acts as a conductor between the electrode and skin. Non-contact electrodes (also known as capacitive electrodes or insulating electrodes) are capacitively coupled; i.e. the ECG signal couples on to the electrodes, even through clothes. Textile electrodes are those made of conductive fabric and can be incorporated into clothing.

Active electrodes are those which have built-in pre-amplification circuits so that they amplify the ECG signal directly after the conductive material.

This section will mainly focus on the two types of dry electrodes.

2.8.2 Comparing dry contact and non-contact/capacitive electrodes against wet electrodes

Dry contact electrodes provide direct contact with the skin, no electrolytic gel and no skin preparation is required. Skin perspiration (sweat) usually replaces the gel [34]. For long-term monitoring applications, they are favoured over wet electrodes as these require electrolytic gel to be constantly present for high-quality recordings. For long-term monitoring, this gel can cause skin irritation and dries up, eventually needing to be continuously reapplied, which is impractical. However, dry electrodes are more challenging as they have a larger skin-electrode or contact impedance.

The literature mainly compares the two types of electrodes against wet electrodes as these are approved for clinical use. Additionally, their properties are well characterised and they have been studied over many decades [34].

There are many factors that need to be considered when dealing with dry contact electrodes such as contact impedance, proneness to motion artefacts and noise performance/the quality of the recorded signal itself. Searle and Kirkup compared wet (Ag/AgCl), dry and insulating electrodes against these factors in [35]. In terms of noise performance, they concluded that the motion artefacts associated with using dry electrodes were significantly higher than that associated with wet electrodes at the beginning of the test. However with time, the effect of these motion artefacts decreased and less noise was present. This was due to the fact that a reduction in skin/electrode interface effects occurs. In a paper researching skin motion artefacts [36], it was shown that there is a slight reduction in skin potential artefact in repetitive tests, however in [35], [37] it is stated that the reduction in motion artefact was due to accumulated perspiration under the electrodes, which effectively acts similar to the gel used in wet electrodes.

Contact impedance

In [35] the same trend was observed with contact impedance. For dry electrodes, the value was initially large (around $10\text{M}\Omega$) and after about 200 seconds the value settled down to around $0.5\text{M}\Omega$. However, the wet electrodes have a lower settling time with a smaller deflection range as well as a lower contact impedance (which is expected) of approximately $0.25\text{M}\Omega$. The cited paper shows graphs of the contact impedance against time for three different types of dry electrodes as well as the wet electrodes. It was therefore demonstrated that after some settling time, the dry electrodes performed

as well as the wet ones. However, these results are only based on two dry electrode implementations. Similar experiments were carried out in [38], [39], [34] and observed a similar trend. Therefore, some settling time is required before dry electrodes can achieve the performance associated with wet electrodes.

A method of overcoming this limitation is to use a high impedance input for the biopotential amplifier, this will prevent any impedance mismatches and any reduction in circuit CMR and performance.

As for capacitive electrodes, it was shown that maximising the resistance in the electrode-skin interface is beneficial in some cases. This is supported by circuit theory which was then validated by experimental data presented in [34].

Noise and motion effects

The paper in [34] also presented noise comparisons between Ag/AgCl wet electrodes, dry contact electrodes and non-contact ones, as well as the recorded ECG signal quality obtained from each. The noise voltage levels were plotted against time. The results showed that the capacitive electrodes were the most prone to noise, followed by the dry contact ones and finally the wet electrodes. However the presence of this noise did not prevent from obtaining acceptable ECG results (for all types of electrodes). The results for dry contact and capacitive electrodes (even when placed over a shirt) showed accurate correspondence when compared to wet electrodes.

In terms of motion effects, motion of the electrodes with respect to the body introduced artefacts when using capacitive and dry electrodes. Capacitive electrodes were found to be the most prone to motion artefacts [34].

Therefore it can be concluded that although dry electrodes do have a limitation of having a 'settling period', they have proven that they provide the same quality ECG recordings as those obtained from using wet electrodes. Although they have a higher contact impedance, this can be overcome by circuit design where a high input impedance should be implemented. Capacitively coupled electrodes provide more freedom and home monitoring as they can record ECG signals over a layer of clothes, however they are most prone to noise introduced by motion artefacts. However, this did not prevent the electrodes from achieving acceptable ECGs.

3 Methods

3.1 Biopotential amplifier design

The biopotential amplifier designed had to meet all the criteria mentioned in sections 2.3.1 and 2.6.2 to successfully record the ECG signal. The block diagram for the developed biopotential amplifier is shown in figure 8. The corresponding circuit schematic is shown in figure 9 with table 1 showing the component values.

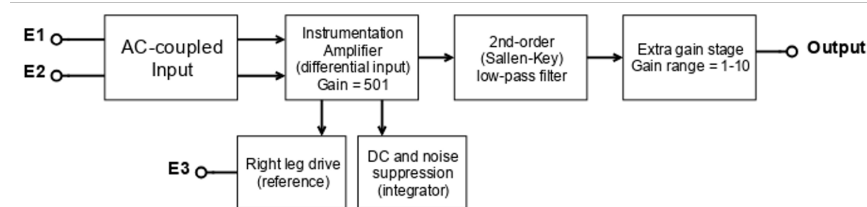


Figure 8: ECG biopotential amplifier block diagram

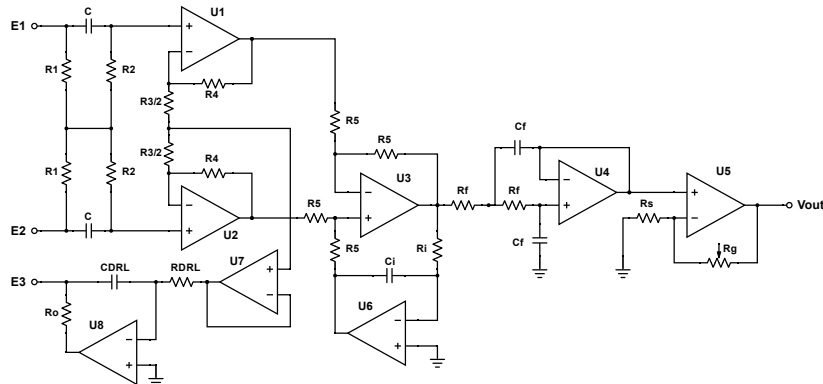


Figure 9: ECG biopotential amplifier circuit schematic

The circuit is based on the design proposed in the Spinelli paper [19] with some modifications and additions. The first stage of the circuit is the ac coupling stage which was discussed in section 2.4. This stage provides coupling for the differential signals as well as a dc path for amplifier bias currents; these drain to ground through the reference electrode [19].

The circuit also acts as a high pass filter with a cut-off of 0.033 Hz, hence providing the necessary high-pass filtering [25]. However, the circuit response time is relatively slow; it can be seen that the time

Table 1: ECG schematic component values

Component	Value
R_1, R_2	$4.7M\Omega$
C	$1\mu F$
R_3	400Ω
R_4	$100k\Omega$
R_5	$47k\Omega$
R_6	$100k\Omega$
R_{DRL}	$10k\Omega$
C_{DRL}	$10nF$
R_o	$510k\Omega$
R_i	$10M\Omega$
C_i	$1\mu F$
R_f	$100k\Omega$
C_f	$10nF$
R_s	$50k\Omega$
R_g	$450k\Omega$
Op. amps	OPA333 [40]

constant, τ , is equal to

$$\tau = R_2 C = 4.7s$$

This is a large value and therefore results in a slow response time. The value of R_2 however is carefully chosen to largely fulfil the requirements in [41] (section A4.2.3.2). The differential signal is then fed to the IA (U1, U2, U3) which provides a differential gain of 501 for the ECG signal.

Although the ac coupling circuit removes dc input voltages, the op-amps input offset voltages are amplified as input signals and this can reduce the output range [19]. There will also be some thermal noise from resistors R_2 and the op-amps input voltage noise. Both these will be amplified which is unwanted. To remove these, the amplifier must reject low-frequency signals, therefore this can be achieved by placing an integrator (op-amp U6) in the feedback loop of the difference amplifier (U3) [19], which also acts as a high-pass filter.

Connected to the common of the IA is a voltage buffer (for impedance matching) which then connects to the DRL circuit. This circuit is connected to the reference electrode and provides common-mode feedback; thus enhancing the circuit's CMMR as discussed in section 2.7.

The next stage in the circuit is a Sallen-Key (2nd order) low-pass filter which is used to attenuate any high-frequency noise as well as any unwanted ECG components. A cut-off of 159 Hz was used. This is obtained using the equation for the cut-off f_c ,

$$f_c = \frac{1}{2\pi R_f C_f}$$

$$f_c = 159 \text{Hz}$$

The final stage in the circuit is an extra-gain stage (a non-inverting setup) which has a gain ranging between 1-10 (implemented using a potentiometer). This stage can be used to provide further gain in case the ECG signal is of small magnitude.

One of the main goals of this project is to develop a miniaturised low-power amplifier, therefore micro-power, micro-sized op-amps are used for this amplifier (OPA333 [40]). The OPA333 also offers excellent CMR as well as a high input impedance.

3.2 PCB design and miniaturisation

A printed circuit board (PCB) was manufactured using the circuit schematic presented in figure 9. Since miniaturisation is a goal of the project, the PCB had to be designed to be as small as possible. Micro-size components were chosen (OPA333 as mentioned above) as well as 0603 pattern resistors and capacitors which are small in size. The PCB design that was tested is shown in appendix A. Unfortunately current circumstances did not allow for a photograph of this PCB, therefore a previous version is included in appendix B as a visual aid - this PCB was smaller as it did not include connectors for the power supplies as in the computer design PCB (top right).

After this PCB successfully recorded ECG signals, a new PCB layout (using the same schematic) was made to further miniaturise the amplifier. This PCB has not been tested, however, the design is shown in appendix C. It is a 4-layer PCB as opposed to the previous one which consists of 2-layers. The first layer includes all the components and signal routing, as well as a ground plane. The 2nd layer is the V_{DD} power plane, the 3rd layer is the V_{SS} power plane and the bottom layer also includes some signal routing and another ground plane. The PCB needs to be tested and verified as the power planes might cause some interference. Otherwise, rearrangement of the layers might need to occur or single supply design can be implemented instead of the current dual supply.

Both PCB designs include BNC connectors which are for testing purposes (coaxial cables will be used for testing the amplifier), therefore the actual amplifier that is being miniaturised is the amplifier itself ignoring the connectors and not the physical PCB dimensions. The amplifier PCB without the BNC connectors is shown in appendix D.

The PCB was powered using a dual power supply of $\pm 1.5V$ (using two 1.5V AAA batteries) where the midpoint was the circuit's ground. The OPA333's minimum power supply is $\pm 0.8V$ therefore this voltage was sufficient.

3.3 Shielding and testing

Since coaxial cables were used, a method of shielding the cables is required in order to clearly record the ECG signal without any external interference. The method of shielding was implemented in the PCB and involves connecting the shields of the coaxial cable inputs (inputs E1, E2 and E3) to the common of the amplifier which is at zero potential (ideally), hence providing a virtual ground for the cable shields. The total gain for the amplifier was 501, with the IA contributing a gain of 501 and the extra gain stage contributing unity gain. Coaxial cables were used for the inputs and for reading the output.

The coaxial cables for the positive, negative and reference inputs were connected to the PCB via the BNC connectors. The cables used are BNC female to dual banana, where the red banana end connects to the signal and the black banana end to the cable shield. The electrode was connected to the red banana via a crocodile clip, and the black banana was left floating as the shielding was already incorporated into the PCB design via the BNC connectors that were soldered. This was done for the three input coaxial cables E1, E2 and E3. The output was connected using a normal coaxial cable; one end on the PCB BNC connector and the other end connecting to the oscilloscope, which was AC coupled. The output coaxial cable was shielded by connecting it to the circuit ground instead of the amplifier common as for E1, E2 and E3.

Normal electrodes with dried gel were used and were attached to crocodile clips connected to the cables.

All carried out tests involve the positive and negative electrodes being placed on the two index fingers. The reason for this choice is that there is a large distance between the two electrodes and this will therefore measure a large magnitude ECG signal, making it more convenient and easier for testing and observing results. Addition-

ally, due to the crocodile clips causing inconsistency in recording the waveform, it was found to be most consistent using two fingers to keep them as still as possible without any metal from the crocodile clips touching the skin and causing distortion. Therefore no clips were touching the subject and the index fingers were positioned on the electrodes themselves.

The reference electrode, E3, is being placed on different parts of the body to compare the results from each. E3 is usually placed on the right leg, this is because of Einthoven's triangle being the by convention. However, the goal of this project is to develop a wireless miniaturised ECG sensor, therefore in future the three electrodes will be very close together (the future concept is shown in section 5; the ECG signal will be of small magnitude in this case) and the reference electrode will not necessarily be on the right leg. It is therefore favourable to test different references to evaluate the performance of the amplifier. As for the small magnitude ECG, the extra gain stage should be adjusted appropriately to account for the smaller signal.

3.4 Lab setup

The setup for testing is shown in figure 10. In the setup, the electrodes are connected to the two index fingers. The output is connected to the oscilloscope (AC coupled) where the results were extracted from the device via a USB stick (data points) and imported on MATLAB to be plotted and manipulated. The test was performed on a healthy 21-year old while at rest.



Figure 10: Lab setup for testing ECG PCB

4 Results and Analysis

4.1 ECG recordings

All graphs shown were obtained from placing the two electrodes (positive and negative electrodes) on the two index fingers with the setup described in sections 3.3 and 3.4. No extra gel was used in any of the recordings except where specified. A total gain of 501 was used for all experiments. The graphs in figure 11 show the results obtained using different right leg drive inputs, i.e. different locations for the reference electrode E3, indicated on the left of each row of graphs. Both the raw data and processed data is shown. The data was processed on MATLAB using the function *smoothdata* where a moving average with a window equal to 60 was used. This means that the data will be smoothed by taking the average over a 60 element sliding window. Beyond this value, the smoothing effect is very ineffective and the amplitude of the QRS complex (the pulses) decreases.

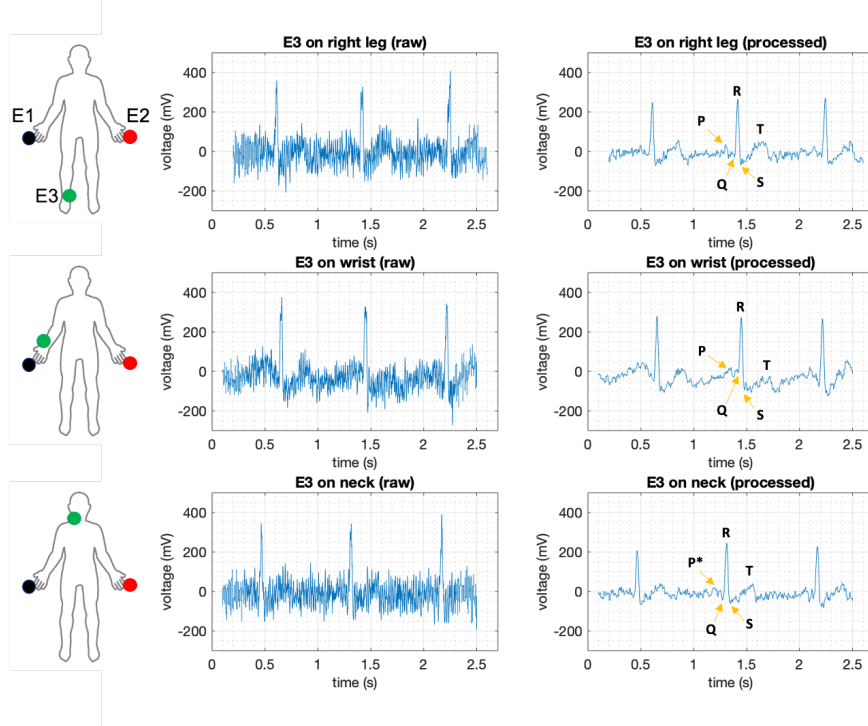


Figure 11: ECG recordings with different E3 inputs (no extra gel used)

Figure 12 shows us the ECG recording when extra conductive gel was used on the electrodes.

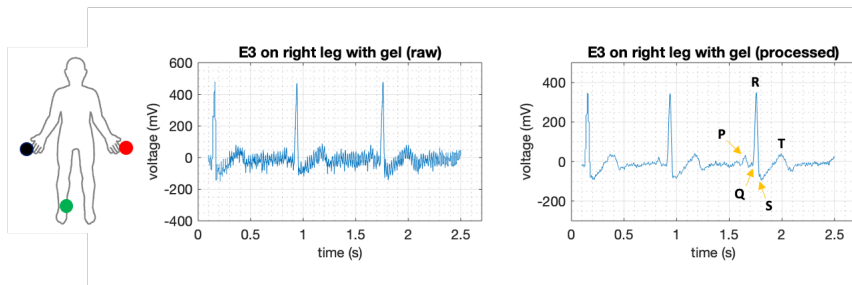


Figure 12: ECG recording with extra gel

4.2 Discussion

4.2.1 ECG waveform characteristics and noise

The waveforms presented in figures 11 and 12 show most aspects of the ideal ECG waveform. In all waveforms the QRS complex is present and clear. The Q-wave is also shown as a negative peak just before the R-wave. The S-wave can also be easily distinguished in all the recordings. Although noise is present, the T-wave can be identified after the QRS complex. As for the P-wave, however, the deflection is present but is almost undistinguishable due to the present noise, even after processing. This statement is aided by the fact that in figure 12, the P-wave is more clear and distinguishable. The T-wave is also less noisy. General signal quality is enhanced in this setup as extra conductive gel was used on the electrodes, hence conductivity was enhanced and noise reduced. In some waveforms in figure 11 the P-wave can be slightly identified, such as in the first and second graphs in figure 11 as shown by the markers on the graphs. In the third graph the P-wave (hence the P^* label) is not very distinguishable as there is more noise present.

However, in the next pulse the P-wave is clearer. There is some inconsistency and this might be because of the pressure applied on the electrodes - the fingers were pressing against the electrodes and therefore the applied pressure is definitely varying slightly throughout the recording period, therefore possibly causing distortion in some aspects of the waveform.

The three graphs represent using different inputs for the DRL circuit (placing the reference electrode E3 on different parts of the body). It can be seen that although using the wrist as the reference provides the least noise (observed from the raw data), when the signal is processed the P-wave is somewhat hidden. Additionally, compared to the other two waveforms, there is more signal baseline drift (against the zero voltage line, known as the isoelectric line). The T-wave for

example should be above the isoelectric line, but in the graph for the wrist reference this is not the case. The right leg and neck reference inputs provide a waveform with less baseline drift.

The noise in the results arises from the cables being used. As previously mentioned, the cables are connected to crocodile clips which attach to the electrodes, therefore not being the most ideal cable connections. Because of this the system was prone to a lot of interference and a lot of noise was introduced in the recordings. The right leg and neck as references had more noise present than the wrist but after signal processing, it was shown that the wrist was the least accurate of the references. Figure 12 was the least prone to this interference because of the use of extra gel.

4.2.2 Waveform amplitudes and frequencies

In figure 11, the raw amplitudes of the QRS complex waves ranges from 300 mV to 400 mV. This is an appropriate level of amplitude for observing ECG signals. After processing, the amplitudes decreased, instead ranging between 200 mV to 300 mV. This is expected as the processing involved a moving average filter. As for figure 12, the raw QRS complex amplitude was approximately 470 mV, with the processed being 340 mV. There is an increased amplitude in this recording as extra gel was used in the setup and increased the electrode-skin conductivity.

As for the frequency of the pulses, the average frequency was equal to approximately 1.2 Hz (a period of 0.829 seconds) which therefore corresponds to a heart rate of 72 bpm (beats per minute). This value falls between the nominal range of the average resting heart rate of adults aged 18-60 (approximately 60-100 bpm) [42].

4.2.3 Further testing and results

In section 3.1 it was shown that the AC coupling circuit had a long response time. For this reason, the AC coupling front was removed so that the positive and negative electrodes pick up the ECG signals and directly feed the signals through two resistors (of magnitude $M\Omega$ s) and into the instrumentation amplifier. The positive and negative terminals were connected to the two index fingers and the reference terminal was connected to the right leg ankle bone. In this setup, the electrodes were removed as using them in the previous configuration did not record an ECG signal. The crocodile clips connected to the wires were held in the palms of the two hands and the reference terminal was pressed against the right leg. No pressure was required for any of the contacts. Using this setup, an ECG signal was recorded.

The resulting waveform was similar to the results shown in figure 11 however the pulses were of lower amplitude (unfortunately, the results were not recorded due to the current COVID-19 situation).

The reason for this amplitude reduction may be due to the lack of ac coupling the ECG signal. When no ac coupling is introduced, dc signals such as electrode offsets can saturate input stages, limiting the gain and reducing the output dynamic range [19], [43] as discussed in section 2.4. The resulting ECG signal is therefore of lower amplitude. This may be the reason why the electrodes had to be removed to record the signal. The signal picked up by the electrodes might have been too weak to be amplified by the limited-gain circuit, therefore better means of contact was required in order to sense the ECG signal. On the other hand, it was observed during the test that the circuit response time was reduced as expected from the theory.

4.2.4 Future testing required

Further testing of the developed design is required before undertaking the next steps in the project. These tests were unfortunately not carried out due to lack of time because of the recent COVID-19 situation.

For example, appropriate tests need to be made with close electrode placement as a method of verifying whether the proposed design is able to amplify small magnitude ECG signals. The extra gain stage was previously set to unity. To test for a small magnitude ECG, this gain might need to be increased to test whether it is a problem of insufficient gain or of flawed circuit design.

The ECG amplifier circuit specifications also need to be tested for and calculated, such as the circuit's overall power consumption, CMMR and signal-to-noise ratio (SNR). Although micro-power components were used to develop the circuit, the exact power consumption has not been computed. A DRL circuit was also used to improve the CMMR, however the exact value also needs computing through appropriate testing.

Lastly, the PCB design in appendix C has not been manufactured yet, therefore the PCB must be manufactured and tested before it is properly implemented in future.

5 Future work

In future, the mini PCB can be integrated with bluetooth technology to allow for wireless transmission of the ECG signal. A design concept shown in figure 13 has been created showing how the overall

system is to be implemented while keeping the miniaturisation and low-power objectives.

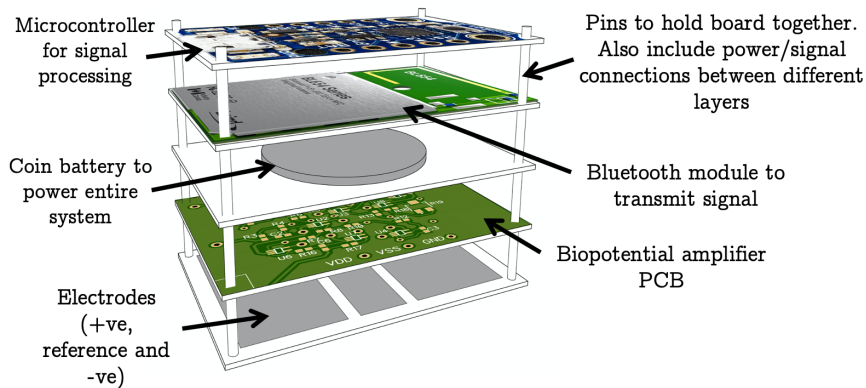


Figure 13: Future miniaturised, wireless ECG amplifier design concept: layers included

The electrodes should be on the underside of the bottom layer but are shown here for clarity. The spacing between the layers has been purposely increased to show the design of each layer, however the final product should be more compact as shown in figure 14.

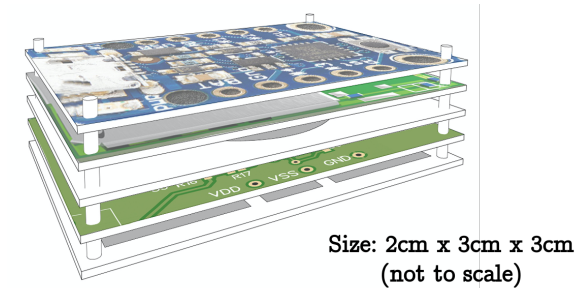


Figure 14: Actual design concept of wireless ECG: compact layers

The design concept provided visualises what the final product could look like. It incorporates the electrodes, the biopotential amplifier, the signal processing, the wireless transmission and the power supply all into one compact mini 5-layer board.

The next immediate tasks to be carried out for improving the design involve carrying out the testing discussed in section 4.2.4. After testing and verifying the design, further steps involve further miniaturising the PCB design and using a single supply to power the board; if a coin watch is to be used only single supply operation is possible. The circuit would then need to be tested using dry

electrodes which are placed closely together as shown in the concept. When the electrodes have been successfully integrated, the signal needs to be sent to the microcontroller for processing (sampling etc.). Finally, the processed signal will need to be transmitted via bluetooth therefore a bluetooth module has to be incorporated in the design. BLE (Bluetooth Low Energy) is the preferred method as it offers micro-power consumption compared to other forms of wireless technologies.

Further future work includes developing several of these compact devices and placing each on a certain location on the body, where each device is independent of the other. Each device would then transmit the local ECG signal recorded and transmit it to a computer which will process these signals; aiming to construct a higher quality ECG waveform that can be used for clinical applications.

6 Conclusion

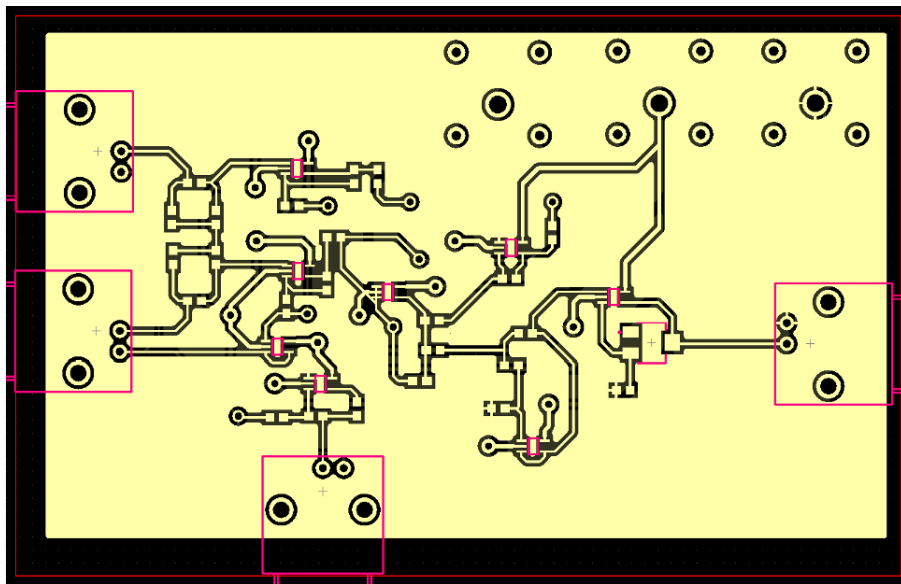
A low-power, miniaturised ECG amplifier PCB was developed and successfully recorded the local ECG signal using different areas of the body for the reference electrode, therefore showing that other areas can be used as the reference. All characteristics of the ideal ECG waveform (P, Q, R, S and T-waves) were clearly observed except in one scenario when the wrist was used for the reference electrode, where the P-wave was slightly undistinguishable from the noise present. With more advanced signal processing techniques, the ECG signal recorded can be cleaner. Despite the circuit's slow response, the absence of the ac coupling stage highlighted the importance of ac coupling in clear acquisition of the QRS complex.

In future, the system is to incorporate dry electrodes as they provide more comfort to patients and are more practical for long-term monitoring. It was found from the literature that after a settling time period, they provide the same quality recordings associated with wet electrodes. The system is also to be integrated with bluetooth technology for wireless transmission, hence a completely wireless solution is to be developed. Although many other approaches developed low-power wireless ECG amplifiers, some wiring is still present and introduces some limitations in terms of set-up and ease of use. The developed amplifier however needs further testing as mentioned in section 4.2.4.

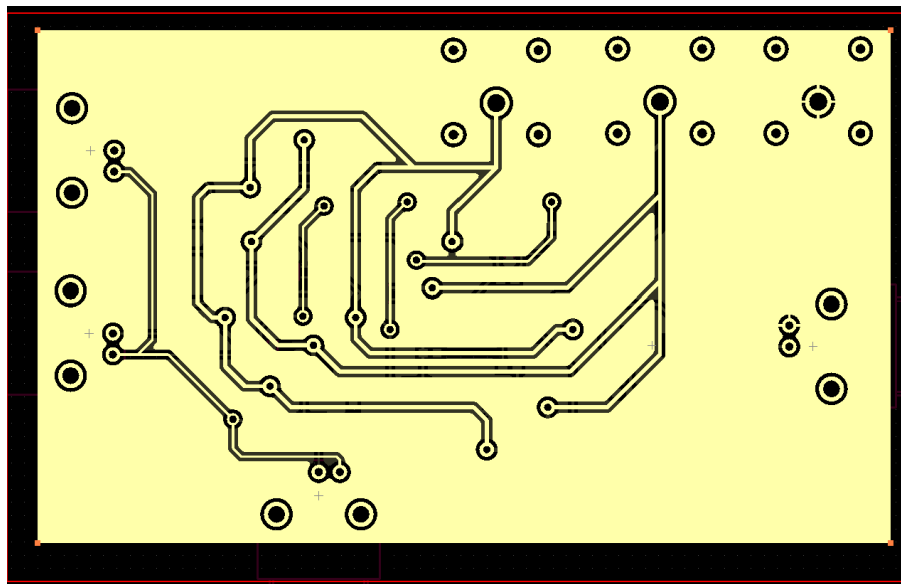
The device is to be integrated with bluetooth technology for wireless transmission of the ECG signal, this objective was not achieved within the time-span of the project. The work done in this project

can be used for future developments towards achieving the miniaturised, fully wireless ECG sensor. A design concept is provided as a start and aid for developing such a system. Future work includes fully developing the 5-layer amplifier, possibly moving on to complete ECG waveform acquisition using several independent amplifiers placed around the body.

A Tested PCB, 2 layer (computer design)

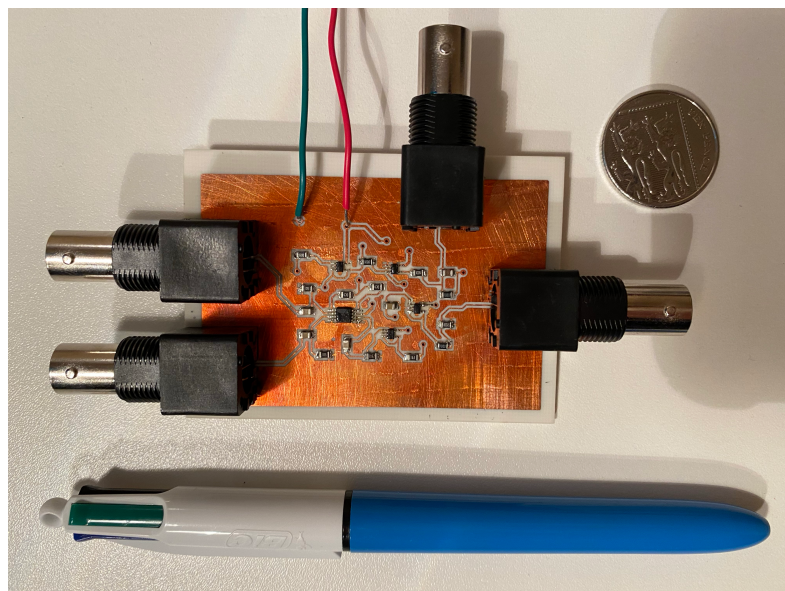


Top layer of PCB. PCB size = 11x7 cm



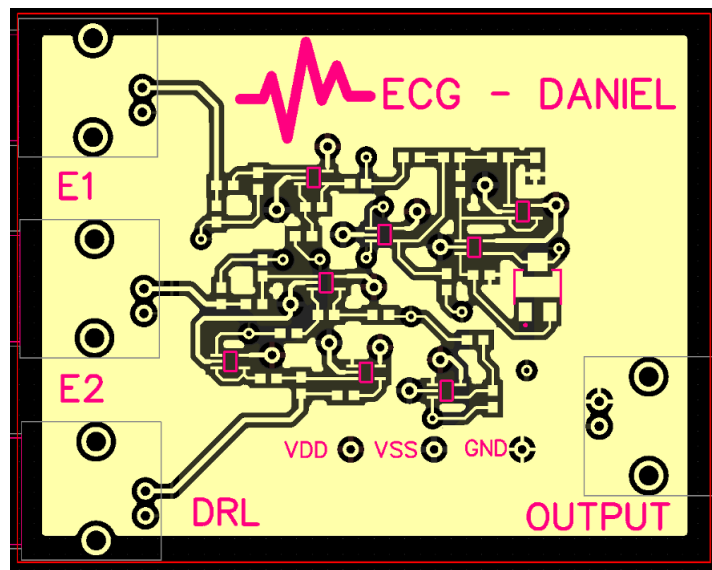
Bottom layer of PCB

B Manufactured PCB (previous version)

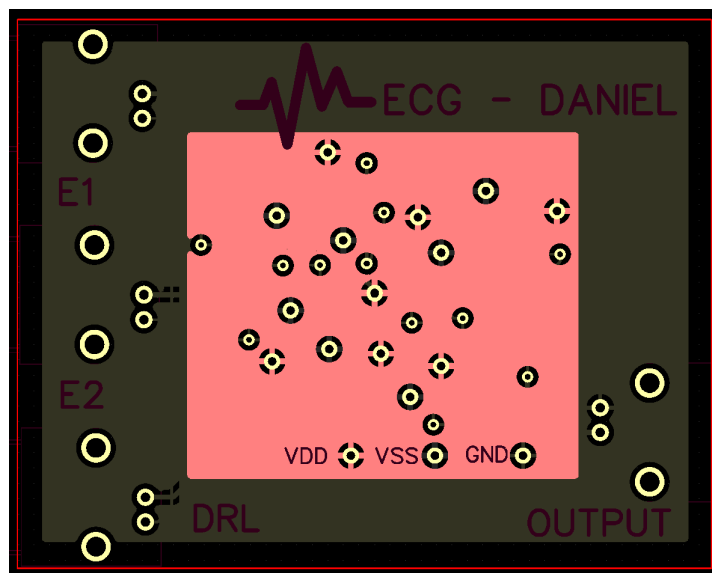


*Manufactured and soldered PCB (previous version) next to pen and
10p coin*

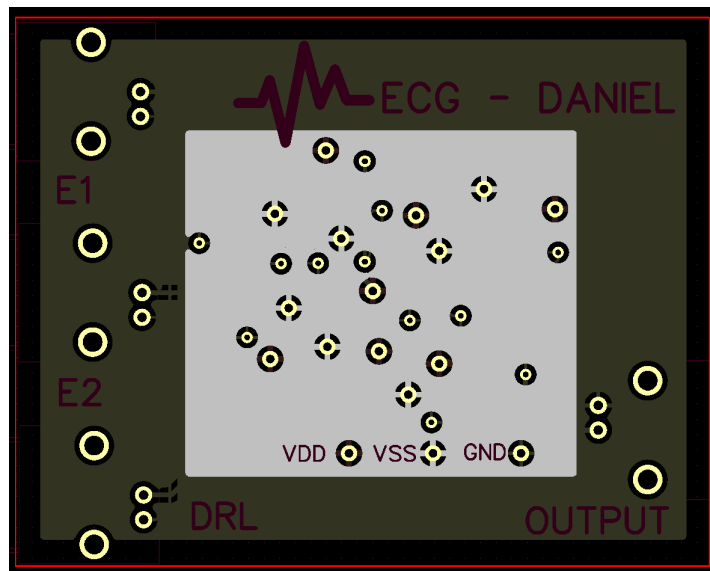
C Miniaturised PCB, 4 layer (computer design)



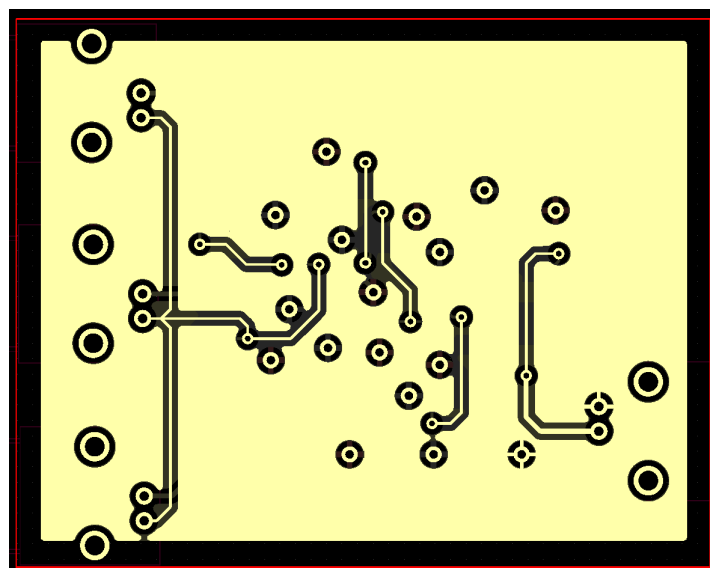
Top layer of PCB. PCB size = 7x5.7 cm



2nd layer of PCB, V_{DD}

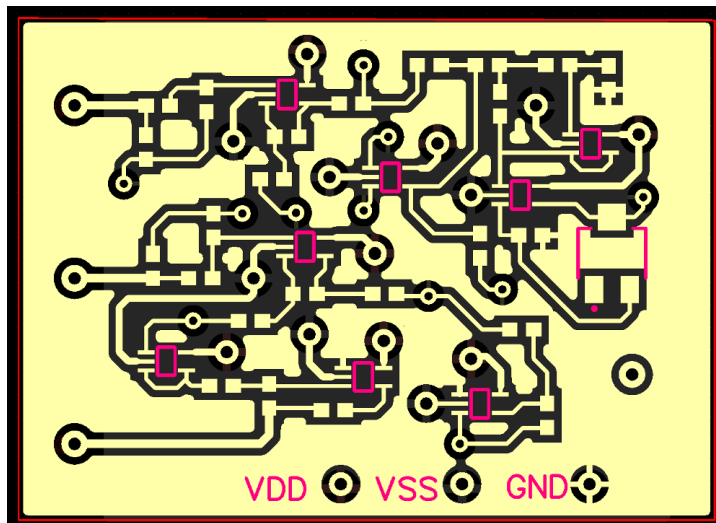


3rd layer of PCB. V_{SS}



Bottom layer of PCB

D Miniaturised PCB without BNCs (actual amplifier size)



PCB without BNC connectors. PCB size = 3.5x5 cm

References

- [1] D. Dias and J. Paulo Silva Cunha, "Wearable health devices-vital sign monitoring, systems and technologies," *Sensors (Basel, Switzerland)*, vol. 18, no. 8, p. 2414, 2018.
- [2] A. JOSHI, A. TOMAR, and M. TOMAR, "A review paper on analysis of electrocardiograph (ecg) signal for the detection of arrhythmia abnormalities," *International Journal of Advanced Research in Electrical, Electronics and Instrumentation Engineering*, vol. 03, pp. 12466–12475, 2014.
- [3] R. Subbiah, L. J. Gula, G. J. Klein, A. C. Skanes, R. Yee, and A. D. Krahm, "Syncope: review of monitoring modalities," *Current cardiology reviews*, vol. 4, no. 1, pp. 41–48, 2008.
- [4] P. Coumel, "Diagnostic and prognostic values and limitations of holter monitoring," *European Heart Journal*, vol. 10, no. suppl E, pp. 19–30, 1989.
- [5] K. V. Olshausen, T. Witt, T. Pop, N. Treese, K.-P. Bethge, and J. Meyer, "Sudden cardiac death while wearing a holter monitor," *The American Journal of Cardiology*, vol. 67, no. 5, pp. 381 – 386, 1991.
- [6] J. Mekoulou, A. N. Peguy Brice, A. Temfemo, A. Tamdja, M. Abanda, C. Bika, E. Tchoudjin, G. Wiliam Richard, L.-G. Gassina, and S. Mandengue, "Pre- and post-exercise electrocardiogram pattern modifications in apparently healthy school adolescents in cameroon," *International journal of adolescent medicine and health*, 2017.
- [7] C.-C. Hsu, B.-S. Lin, K.-Y. He, and B.-S. Lin, "Design of a wearable 12-lead non-contact electrocardiogram monitoring system," *Sensors*, vol. 19, no. 7, p. 1509, 2019.
- [8] A. Boehm, X. Yu, W. Neu, S. Leonhardt, and D. Teichmann, "A novel 12-lead ecg t-shirt with active electrodes," *Electronics*, vol. 5, no. 4, p. 75, 2016.
- [9] E. Nemati, M. Deen, and T. Mondal, "A wireless wearable ecg sensor for long-term applications," *IEEE Communications Magazine*, vol. 50, pp. 36–43, 2012.
- [10] G. Gargiulo, P. Bifulco, M. Cesarelli, M. Ruffo, M. Romano, R. A. Calvo, C. Jin, and A. van Schaik, "An ultra-high input impedance ECG amplifier for long-term monitoring of athletes," *Medical devices (Auckland, N.Z.)*, vol. 3, pp. 1–9, 2010.

- [11] V. P. Rachim and W. Chung, "Wearable noncontact armband for mobile ecg monitoring system," *IEEE Transactions on Biomedical Circuits and Systems*, vol. 10, no. 6, pp. 1112–1118, 2016.
- [12] J. Coosemans, B. Hermans, and R. Puers, "Integrating wireless ecg monitoring in textiles," in *The 13th International Conference on Solid-State Sensors, Actuators and Microsystems, 2005. Digest of Technical Papers. TRANSDUCERS '05.*, vol. 1, pp. 228–232 Vol. 1, 2005.
- [13] J. Ottenbacher, S. Romer, C. Kunze, U. Grossmann, and W. Stork, "Integration of a bluetooth based ecg system into clothing," in *Eighth International Symposium on Wearable Computers*, vol. 1, pp. 186–187, 2004.
- [14] J. Malmivuo and R. Plonsey, *Bioelectromagnetism - Principles and Applications of Bioelectric and Biomagnetic Fields*. 1995.
- [15] D. E. Becker, "Fundamentals of electrocardiography interpretation," *Anesthesia Progress*, vol. 53, no. 2, pp. 53–64, 2006.
- [16] J. Nagel, *Biopotential Amplifiers*. 1999.
- [17] E. Ryzhii, "Computer simulation of cardiac electrical activity by three-dimensional whole heart and heterogeneous oscillator models," 2017.
- [18] F. Zhang, J. Holleman, and B. P. Otis, "Design of ultra-low power biopotential amplifiers for biosignal acquisition applications," *IEEE Transactions on Biomedical Circuits and Systems*, vol. 6, no. 4, pp. 344–355, 2012.
- [19] E. M. Spinelli, R. Pallas-Areny, and M. A. Mayosky, "Accoupled front-end for biopotential measurements," *IEEE Transactions on Biomedical Engineering*, vol. 50, no. 3, pp. 391–395, 2003.
- [20] R. Pallas-Areny and J. G. Webster, "Common mode rejection ratio in differential amplifiers," *IEEE Transactions on Instrumentation and Measurement*, vol. 40, no. 4, pp. 669–676, 1991.
- [21] M. Blanco-Velasco, B. Weng, and K. E. Barner, "ECG signal denoising and baseline wander correction based on the empirical mode decomposition," *Computers in Biology and Medicine*, vol. 38, no. 1, pp. 1 – 13, 2008.
- [22] S. Wan and H. Nguyen, "50 Hz interference and noise in ECG recordings – a review," *Australasian physical and engineering sciences in medicine / supported by the Australasian College of Physical Scientists in Medicine and the Australasian Association of Physical Sciences in Medicine*, vol. 17, pp. 108–15, 1994.

- [23] P. Gupta, K. K. Sharma, and S. D. Joshi, "Baseline wander removal of electrocardiogram signals using multivariate empirical mode decomposition," *Healthcare technology letters*, vol. 2, no. 6, pp. 164–166, 2015.
- [24] J. J. Bailey, A. S. Berson, A. Garson, L. G. Horan, P. W. Macfarlane, D. W. Mortara, and C. Zywietz, "Recommendations for standardization and specifications in automated electrocardiography: bandwidth and digital signal processing," *Circulation*, vol. 81, no. 2, pp. 730–739, 1990.
- [25] C. E. Kossmann, D. A. Brody, G. E. Burch, H. H. Hecht, F. D. Johnston, C. Kay, E. Lepeschkin, H. V. Pipberger, H. V. Pipberger, G. Baule, A. S. Berson, S. A. Briller, D. B. Geselowitz, L. G. Horan, and O. H. Schmitt, "Recommendations for standardization of leads and of specifications for instruments in electrocardiography and vectorcardiography," *Circulation*, vol. 35, no. 3, pp. 583–602, 1967.
- [26] F. Buendía-Fuentes, M. A. Arnau-Vives, A. Arnau-Vives, Y. Jiménez-Jiménez, J. Rueda-Soriano, E. Zorio-Grima, A. Osasáez, L. V. Martínez-Dolz, L. Almenar-Bonet, and M. A. Palencia-Pérez, "High-bandpass filters in electrocardiography: Source of error in the interpretation of the st segment," *ISRN Cardiology*, 2012.
- [27] G.-N. J. Parola F, "Use of high-pass and low-pass electrocardiographic filters in an international cardiological community and possible clinical effects," *Adv J Vasc Med*, 2017.
- [28] P. Kligfield, L. S. Gettes, J. J. Bailey, R. Childers, B. J. Deal, E. W. Hancock, G. van Herpen, J. A. Kors, P. Macfarlane, D. M. Mirvis, O. Pahlm, P. Rautaharju, and G. S. Wagner, "Recommendations for the standardization and interpretation of the electrocardiogram," *Journal of the American College of Cardiology*, vol. 49, no. 10, pp. 1109–1127, 2007.
- [29] D. Ricciardi, I. Cavallari, A. Creta, G. D. Giovanni], V. Calabrese, N. D. Belardino], S. Mega, I. Colaiori, L. Ragni, C. Proscia, A. Nenna, and G. D. Sciascio], "Impact of the high-frequency cutoff of bandpass filtering on ecg quality and clinical interpretation: A comparison between 40hz and 150hz cutoff in a surgical preoperative adult outpatient population," *Journal of Electrocardiology*, vol. 49, no. 5, pp. 691 – 695, 2016.
- [30] B. B. Winter and J. G. Webster, "Driven-right-leg circuit design," *IEEE Transactions on Biomedical Engineering*, vol. BME-30, no. 1, pp. 62–66, 1983.

- [31] A. C. M. van Rijn, A. Peper, and C. Grimbergen, "High-quality recording of bioelectric events," *Medical and Biological Engineering and Computing*, vol. 29, no. 4, pp. 433–440, 1991.
- [32] A. G. Webb, *Principles of Biomedical Instrumentation*. Cambridge Texts in Biomedical Engineering, Cambridge University Press, 2018.
- [33] M. Guermandi, E. F. Scarselli, and R. Guerrieri, "A driving right leg circuit (dgrl) for improved common mode rejection in bio-potential acquisition systems," *IEEE Transactions on Biomedical Circuits and Systems*, vol. 10, no. 2, pp. 507–517, 2016.
- [34] Y. Chi, T.-P. Jung, and G. Cauwenberghs, "Dry-contact and noncontact biopotential electrodes: Methodological review," *Biomedical Engineering, IEEE Reviews in*, vol. 3, pp. 106 – 119, 02 2010.
- [35] A. Searle and L. Kirkup, "A direct comparison of wet, dry and insulating bioelectric recording electrodes," *Physiological measurement*, vol. 21, pp. 271–83, 06 2000.
- [36] H. de Talhouet and J. G. Webster, "The origin of skin-stretch-caused motion artifacts under electrodes," *Physiological Measurement*, vol. 17, pp. 81–93, may 1996.
- [37] N. Meziane, J. Webster, M. Attari, and A. Nimunkar, "Dry electrodes for electrocardiography," *Physiological measurement*, vol. 34, pp. R47–R69, 08 2013.
- [38] L. Geddes and M. Valentinuzzi, "Temporal changes in electrode impedance while recording the electrocardiogram with "dry" electrodes," *Annals of biomedical engineering*, vol. 1, pp. 356–67, 04 1973.
- [39] M. S. SPACH, R. C. BARR, J. W. HAVSTAD, and E. C. LONG, "Skin-electrode impedance and its effect on recording cardiac potentials," *Circulation*, vol. 34, no. 4, pp. 649–656, 1966.
- [40] Texas Instruments, *OPA333 1.8V, 17 μ A, microPower, precision, zero-drift CMOS op amp*, 2006. Rev. E.
- [41] Association for the Advancement of Medical Instrumentation, *Ambulatory electrocardiographs*. 1998.
- [42] R. Avram, G. H. Tison, K. Aschbacher, P. Kuhar, E. Vittinghoff, M. Butzner, R. Runge, N. Wu, M. J. Pletcher, G. M. Marcus, and J. Olglin, "Real-world heart rate norms in the health eheart study," *NPJ digital medicine*, vol. 2, pp. 58–58, 2019.
- [43] E. M. Spinelli, N. Martinez, M. A. Mayosky, and R. Pallas-Areny, "A novel fully differential biopotential amplifier with

dc suppression," *IEEE Transactions on Biomedical Engineering*, vol. 51, no. 8, pp. 1444–1448, 2004.